VIP Anisotropic Nanostructures

DOI: 10.1002/anie.200702570

Synthesis of Heterodimeric Sphere–Prism Nanostructures via Metastable Gold Supraspheres**

*Rafal Klajn, Anatoliy O. Pinchuk, George C. Schatz, and Bartosz A. Grzybowski**

Noble-metal nanoparticles of nonspherical shapes are interesting for their size- and shape-dependent optical properties[1] and for potential applications in hyperthermia of tumors,[2] pathogen detection,[3] and infrared-absorbing coatings.[4] Typically, such particles are grown in the presence of surfactants that stabilize certain crystallographic faces. For example, silver nanocubes can be prepared by stabilizing the Ag {100} faces with poly(4-vinylpyrrolidone) (PVP),[5] while gold nanorods are grown readily in the presence of cetyltrimethylammonium bromide (CTAB), which adsorbs selectively onto Au {100} faces.[6] Other nanostructures prepared by the latter method include gold hexagons,[7–9] gold triangles,[10–12] silver disks,[13] and several other shapes.[14] Recently, considerable effort has been devoted to the preparation of hybrid or dimer nanostructures, in which two (or more) domains of different shapes or material properties are permanently connected.[15] Such structures are usually made by epitaxial nucleation and growth on presynthesized nanoparticle seeds[16,17] or by thermal decomposition of core–shell nanoparticles.[18] Herein, we describe a conceptually different route to a new class of nanoscopic heterodimers composed of spherical and polygonal domains. In our method, individual nanoparticles (NPs) are first assembled into metastable, supraspherical aggregates (SS, Figure 1a,b), and are then thermally decomposed into heterodimers (Figure 2). These composite particles are the result of temperature-induced coalescence of individual NPs accompanied by crystal nucleation. During this process, the relative sizes and dimensions of the SS and crystalline domains change controllably and give rise to pronounced changes in the particles' optical response.

In a typical experiment, gold supraspheres (SS, diameter 96 ± 13 nm[19–23]) were prepared by rapid addition of 1,8-octanedithiol dissolved in toluene (2.86 mM, 40 μL) to a stirred solution of gold nanoparticles ($c_{Au} = 1.0$ mM, 1.75 mL) stabilized in toluene by excess didodecyldimethylammonium bromide (DDAB, 9 mM) and dodecylamine (DDA, 20 mM; Figure 1a,b). The dithiol molecules displaced a portion of the loosely bound surfactant molecules and simultaneously cross-linked the NPs. The cross-linking continued until all NPs in solution were aggregated into spherical aggregates (SS), each composed of approximately 2500 NPs and with an average of 150 dithiol ligands per NP (for details of the growth mechanism, see reference [21]).

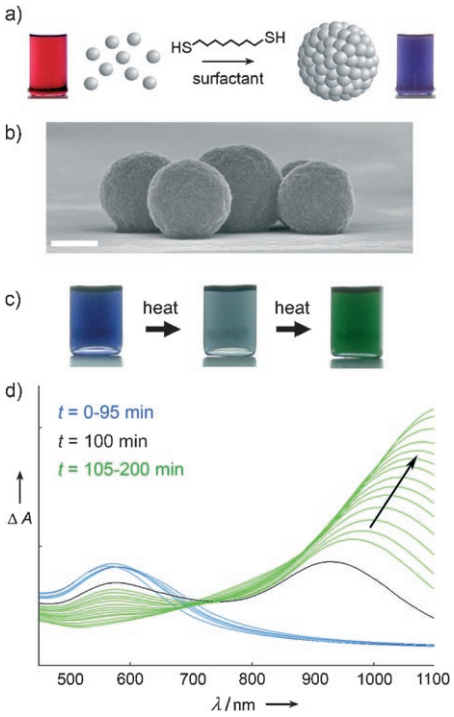

Figure 1. a) Preparation of Au SS by controlled cross-linking of gold nanoparticles. The transformation is accompanied by a pronounced color change. b) SEM side view of several supraspheres resting on a surface of silicon. Scale bar = 100 nm. c) Color changes observed during thermal treatment of Au SS at 95 °C. d) UV/Vis spectra of the reaction mixture recorded at different heating times *t*. The spectra change abruptly at around 100 min.

When the SS solution was heated at 95 °C, it remained blue for times $t < 100$ min, then rapidly turned gray; subsequently, its color slowly changed to green ($t \approx 100$–200 min, Figure 1c). Corresponding UV/Vis spectra showed that at around $t = 100$ min, the intensity of the SS surface plasmon resonance (SPR) band at $\lambda_{max} = 580$ nm decreased dramatically, while a new, strong band at $\lambda_{max} = 920$ nm appeared

[*] Dipl.-Chem. R. Klajn, Dr. A. O. Pinchuk, Prof. Dr. G. C. Schatz, Prof. Dr. B. A. Grzybowski
Department of Chemical and Biological Engineering and Department of Chemistry
Northwestern University
2145 Sheridan Rd., Evanston, IL 60208 (USA)
Fax: (+1) 847-491-3024
E-mail: grzybor@northwestern.edu
Homepage: http://www.dysa.northwestern.edu

[**] This work was supported by the NSF CAREER (CTS-0547633) Award, 3M NTF Award, the Pew Scholarship in the Biomedical Sciences and the Sloan Fellowship (to B.A.G.). R.K. and A.O.P. were supported by NSF under the Northwestern MRSEC (DMR-0520513). R.K. would like to thank Dr. Alexander Kalsin and Paul Wesson for helpful discussions. DDA calculations were performed using the DDSCAT.6.1 program, available free of charge at http://www.astro.princeton.edu/~draine/DDSCAT.html.

Supporting information for this article is available on the WWW under http://www.angewandte.org or from the author.

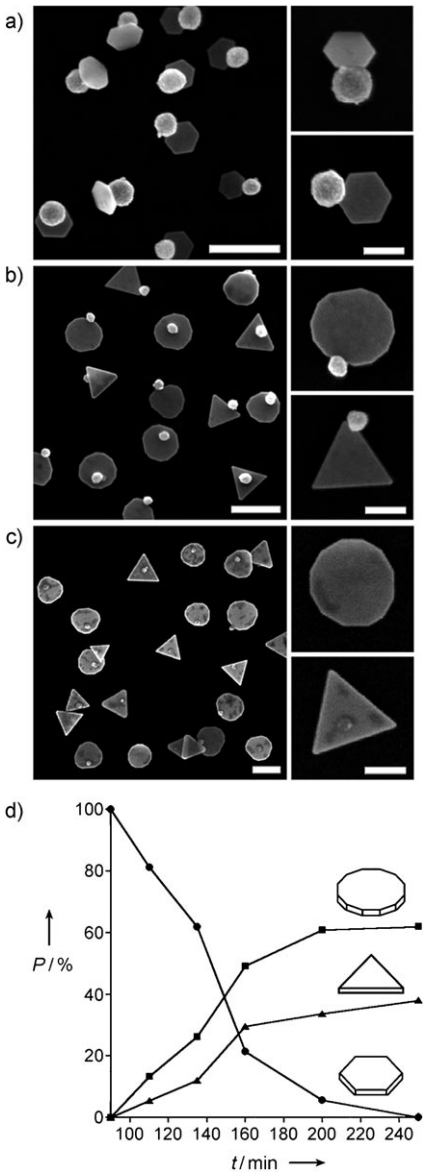

Figure 2. SEM images of Au SS transforming into prisms at 95 °C. Reaction was quenched after a) 110 min, b) 190 min and c) 250 min. Scale bars correspond to 200 nm (left panels) and 100 nm (right panels). d) Proportions of particles (*P*) of different morphologies at different heating times at 95 °C.

(Figure 1 d). Further heating caused the intensity of this new band to increase and its position to shift to higher wavelengths. These changes were accompanied by a gradual decrease in the intensity of the $\lambda_{max} = 580$ nm band. No further changes were observed after $t \approx 250$ min.

To study structural evolution of the SS during heating, we terminated the process at different times by rapidly lowering the temperature to 25 °C while evaporating the solvent. Scanning electron microscopy (SEM) images showed that for $t < 100$ min, the morphologies of the SS aggregates did not change. However, at $t \approx 100$ min, each suprasphere "budded" a hexagonal plate on its surface (Figure 2 a). Upon further heating, these hybrid structures evolved into suprasphere connected to either triangles or dodecagons (Figure 2 b). During this evolution, the plates grew at the expense of the SS. At every stage of this process, the standard deviation in the sizes of the plate domains was up to approximately 20 %, and the average volume and mass of the dimers remained roughly constant, suggesting that these structures evolved but did not merge with one another (see the Supporting Information, Section 1). Ultimately, at $t \approx 200$ min, the spheres disappeared completely to give a mixture of triangular and dodecagonal prisms (Figure 2 c, d). High-resolution TEM images of the particles taken at different times showed that the plate domains had no structural defects in the {111} planes (Figure 3). The single-crystalline nature of the plates was confirmed by selected-area electron diffraction (SAED) patterns taken perpendicular to the {111} face (Figure 3 c).

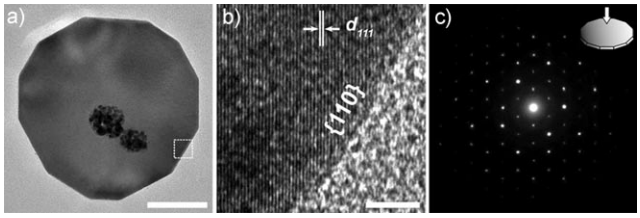

Figure 3. a) TEM image of a typical dodecagon. b) High-resolution image of the area in (a) delineated by a white frame. The measured lattice constant of the {111} face is 2.4 Å and in good agreement with that of bulk Au {111} (2.355 Å). Scale bars = 50 nm in (a) and 5.0 nm in (b). c) SAED diffraction pattern taken perpendicular to the {111} face of a dodecagonal plate (see inset).

The progress of the sphere-to-heterodimer transformation was affected by temperature, by the presence and types of the surfactants stabilizing the supraspheres,[24,25] and by the concentration of dithiol cross-linkers. Specifically, below 85 °C, SS were stable for several days and did not nucleate any crystals. At 90 °C, "budding" of small crystals started only after $t \approx 200$ min, and it took roughly 6 h to obtain pure but relatively polydisperse crystals (triangles and dodecagons) without any SS present. Interestingly, a small percentage (1–2 %) of the heated SS nucleated two crystals (see the Supporting Information, Figure S2). Finally, at 100 °C, the SS precipitated from the solution rapidly and formed an extended porous network structure.

When the spheres were purified from excess of DDA and DDAB surfactants,[26] heating at 95 °C caused their rapid ($t <$ 10 min) precipitation into a network-like structure (see the Supporting Information, Figure S3a). When, however, the concentration of DDA was adjusted to its original value (20 mM), the SS heated at 95 °C remained stable in solution for several days and did not bud any crystals (though some of the NPs in the SS coalesced, see the Supporting Information, Figure S3b). Finally, with no DDA and only DDAB present (9 mM), the SS heated at 95 °C precipitated rapidly ($t \approx 15$ min) to give a mixture of polydisperse plates of various morphologies, including tetrahedra, triangles, and higher polygonal plates (see the Supporting Information, Figure S3c).

Overall, these experiments suggest that: i) Evolution of supraspheres is driven by desorption of the molecules coating

the individual nanoparticles and by the coalescence of these particles.[27] In particular, the optimal temperature for heterodimer synthesis (95 °C) coincides with the previously measured (by DSC[28]) threshold temperature of alkyl thiol desorption from AuNPs. This finding suggests that removal of tightly bound dithiol ligands is a necessary condition for efficient NP coalescence. ii) An excess of DDA surfactant stabilizes the supraspheres and prevents their aggregation. This effect can be attributed to the surfactant lowering the dielectric contrast between the SS and the solvent and thus lowering the magnitudes of van der Waals attractions between the supraspheres.[22] iii) DDAB controls the growth of the budded crystals by stabilizing {111} crystallographic facets of gold.[29–31] Once a hexagonal seed bound by two {111} planes forms, adatoms have difficulty attaching to these flat planes,[32] and the crystal grows sideways. Indeed, we verified experimentally that the thickness of the growing crystalline polygons does not change during in the entire course of SS evolution (e.g. 9.5 ± 1.5 nm for the conditions discussed above). However, for given concentrations of DDAB and DDA, the plate thickness depends on and can be regulated by the ratio of the concentration of dithiol cross-linkers to the concentration of nanoparticles, $x = [\mathrm{DT}]/[\mathrm{NP}]$. When x is low, all dithiols desorb rapidly, and the supraspheres bud large, thin plates (e.g. 6 nm thick for $x \approx 86$). When x is high, the SS-to-dimer transition takes much longer, and the coalescing NPs are still held together by the dithiols not fully desorbed from the supraspheres. As a result, the plates are more compact and up to 50 nm thick (for $x \gtrsim 800$). These trends are quantified in Figure 4.

The evolution of the heterodimers' hexagonal domains into triangles can be explained by the differences in the growth rates of various crystallographic faces. Specifically, transformation of hexagons into triangles is similar to that observed in other systems[32,33] and is due to the fact that the alternating {100} faces along the hexagon's perimeter have higher surface energies[34] and grow more rapidly than the {111} faces. Transformation of hexagons into dodecagons is a more complex process (Figure 5a) that begins with the formation of three {110} crystal faces at three alternate corners of a hexagon (Figure 5b)[35] with subsequent formation of three other {110} faces at the remaining corners (Figure 5c). Although the {110} faces are relatively unstable because of the associated large interatomic distances,[36] their formation is facilitated by high local concentration of the desorbing dithiols, which are known to bind to Au {110} with the highest affinity.[37] Once the {110} faces nucleate, their growth over both {111} and {100} is preferred and leads to dodecagons. Interestingly, if {110} faces nucleate later, during transformation of hexagons into triangles, the triangles become truncated (Figure 5a,e) and ultimately evolve into non-equilateral dodecagons (Figure 5a,f), which are sometimes seen in the reaction mixture.

Finally, we discuss the optical properties of the heterodimeric particles, whose UV/Vis spectra reflect the structures of individual domains. These spectra are well approximated by a linear superposition of the optical responses of the supraspheres and of the crystalline plates. To model the extinction of the SS domains (see the Supporting Information), we used the Maxwell–Garnett (MG) theory, which is an effective-medium approach to inhomogeneous mixtures of two or more phases having different dielectric constants (e.g. colloidal solutions of metal NPs). For the polygonal plates, we applied the discrete dipole approximation,[38] which can accurately describe optical properties of

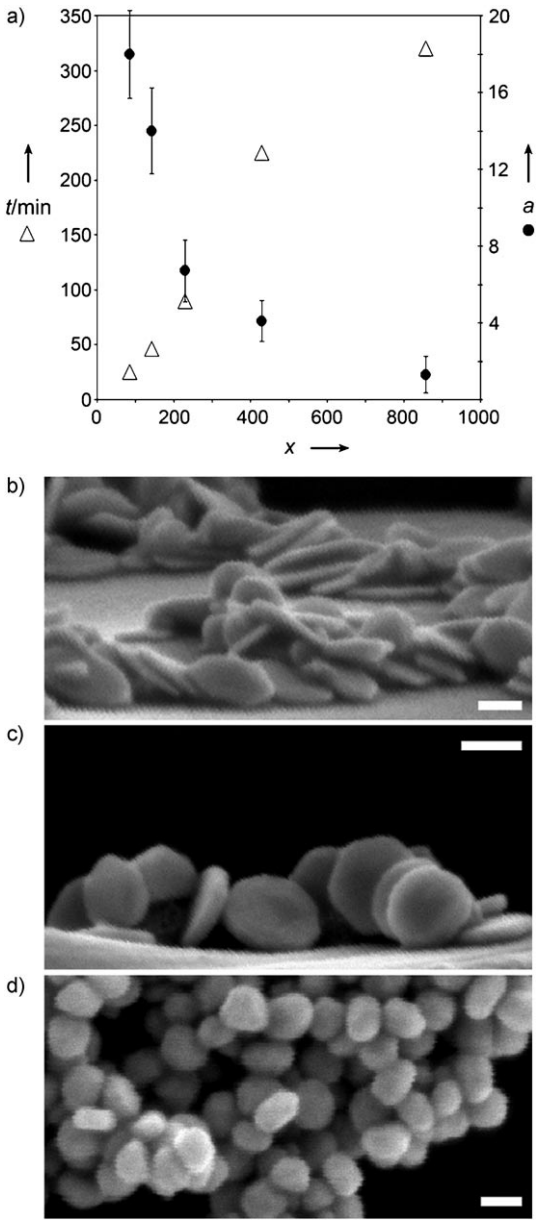

Figure 4. a) Aspect ratios a (i.e. plates' width to thickness, ●) and heating times at 95 °C (t, △) before the onset of budding for plates obtained from similarly sized (ca. 96-nm) supraspheres differing in the number of dithiol cross-linkers per nanoparticle, $x = [\mathrm{DT}]/[\mathrm{NP}]$. Supraspheres that are less cross-linked nucleate plates early (e.g. 40 min for $x = 86$); when $x \gtrsim 800$, the SS need to be heated for more than five hours. The aspect ratios of the final plates (i.e. when supraspheres disappear completely), decrease with increasing x. The SEM images show b) thin plates (thickness ca. 6 nm, $a \approx 18.0$) obtained from $x = 86$ supraspheres; c) intermediate plates (thickness ca. 11 nm, $a \approx 6.7$) from $x = 229$ SS; and d) compact plates (thickness ca. 40 nm, $a \approx 1.23$) from $x = 860$ SS. All scale bars correspond to 50 nm.

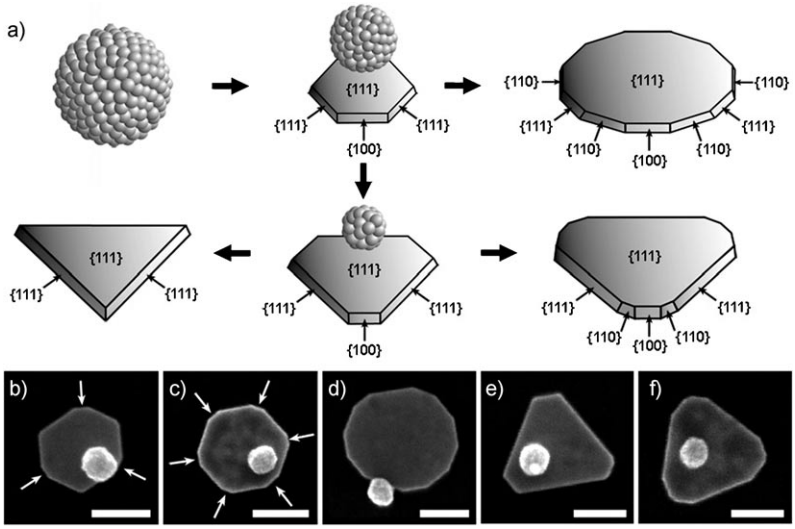

Figure 5. a) Schematic representation of thermally-induced transformation of Au SS in the presence of DDA and DDAB. Initially, the supraspheres bud hexagonal crystals. These hexagons grow either by the addition of adatoms to the {100} faces, leading to triangles (bottom left) or, if {110} faces appear at each of the hexagon's corners, transform into dodecagon (top right). In a much less common scenario, {110} faces form in an intermediate structure (truncated triangle), which then gives rise to an extended dodecagon (bottom right). Different stages of this evolution are captured in SEM images shown in (b)–(f). b) Evolution to dodecagons begins with the formation of three {110} faces (indicated by white arrows) at alternate corners of hexagons. c) Next, three new {110} faces form at the remaining corners (indicated by white arrows). d) An approximately equilateral dodecagon. e) A truncated triangle as an intermediate between a hexagon and a triangle. f) A non-equilateral dodecagon evolved from a truncated triangle. All scale bars correspond to 100 nm.

arbitrarily shaped objects by representing them as a collection of point dipoles.[38] The combination of these two methods gives theoretical spectra that agree with those recorded in experiments (Figure 6). In these spectra, the band at $\lambda_{max} \approx 560$ nm originates from the collective SPR of AuNPs constituting the SS; $\lambda_{max} \approx 920$ nm (for hexagons) and 1050 nm (for triangles and dodecagons) are the in-plane dipole bands, and $\lambda_{max} \approx 800$ nm is a quadrupole peak (barely resolved in the experimental spectrum). The broadness of these peaks reflects the approximately 20% polydispersity of the plate domains, while the red shift of the in-plane bands is attributed to snipping or rounding of the prisms' corners.[25]

In conclusion, we described thermal synthesis of heterodimeric nanostructures by gradual decomposition of supraspherical precursors. Unlike molecular syntheses, this nanoscale transformation allows for the isolation of a continuous range of intermediates between the SS substrates and polygonal-plate products. It offers a high degree of control over the dimensions of each of the dimer's domains and produces particles with tunable optical properties. In the future, it could be extended to structures made of different materials or material combinations. In the latter context, decomposition of SS comprising NPs of several types[21] could lead to hybrid structures, in which the connected domains would vary both in shape and in elemental composition, thus making them suitable anisotropic building blocks for the emerging field of nanochemistry.[39]

Experimental Section

Preparation of nanoparticles: Didodecyldimethylammonium bromide (DDAB, 925 mg) was dissolved in toluene (20 mL) to make a 100 mM stock solution. Tetrachloroauric acid trihydrate ($HAuCl_4 \cdot 3H_2O$, 50 mg) and dodecylamine (DDA, 450 mg) were added to the DDAB stock solution (12.5 mL) and dissolved by sonication. Tetrabutylammonium borohydride (TBAB, 125 mg) dissolved in the DDAB stock solution (5 mL) was added to this mixture dropwise under vigorous stirring. The obtained solution was left to age for 24 h. The aged solution (7 mL) was then added to toluene (50 mL) containing $HAuCl_4 \cdot 3H_2O$ (200 mg), DDAB (1.00 g), and DDA (1.85 g). Finally, hydrazine (131 μL) in the stock solution (20 mL) was added dropwise under vigorous stirring. The procedure gave gold nanoparticles of average diameter $\langle d \rangle = 5.6 \pm 0.50$ nm.

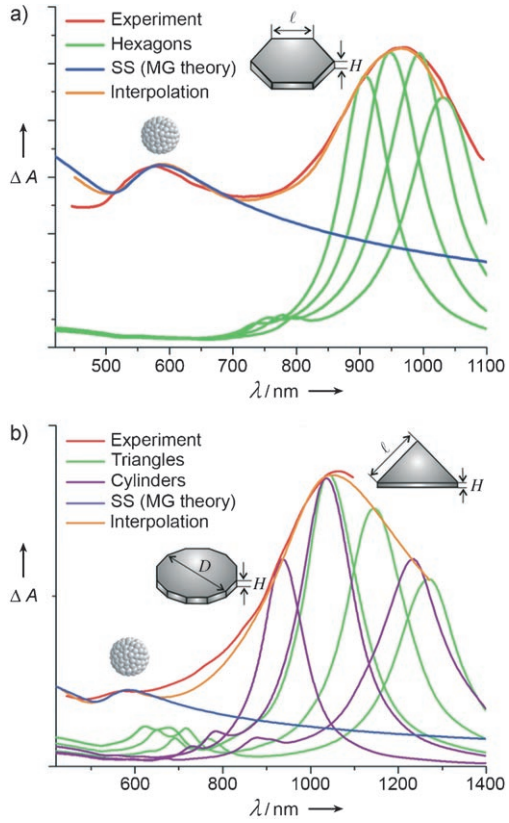

Figure 6. Experimental and theoretical UV/Vis spectra of heterodimers. a) The spectrum of hexagon–suprasphere heterodimers taken after 100 min of heating at 95 °C (red) agrees with the calculated one (interpolation, orange). This interpolation was obtained by linear superposition of component spectra of the supraspheres and a family of spectra corresponding to hexagonal plates of thickness $H = 10$ nm and edge length (from left to right) $l = 50$ nm, 55 nm, 60 nm, 65 nm. Accounting for different plate dimensions reflects the experimentally observed polydispersity of the heterodimers. b) Spectrum modeled for $t = 190$ min is a superposition of individual spectra of supraspheres (blue), triangles ($H = 10$ nm, green), and dodecagons ($H = 10$ nm, violet), the latter two taken in proportions observed experimentally (38% and 62%, respectively). In the calculations, dodecagons are approximated as cylinders. To account for experimental polydispersity, the spectra of triangles were modeled for edge-length l (from left to right) 100 nm, 125 nm, and 150 nm; diameters D of the cylinders were (from left to right) 100 nm, 125 nm and 150 nm.

Preparation of gold supraspheres: A solution of 1,8-octanedithiol solution (400 μL, $c = 2.86$ mM) was added under vigorous stirring to an as-prepared solution of gold nanoparticles (2.5 mL) diluted with toluene (15 mL). The reaction mixture changed color from red to purple within 1 min. The procedure gave Au SS of average diameter $\langle d \rangle = 96 \pm 13$ nm.

Purification of supraspheres: As-prepared SS were purified from DDAB (8.8 mM) and DDA (19.9 mM) by controlled precipitation induced by the addition of methanol (20 vol%). Black precipitate was collected and dissolved in the original volume of toluene. The purification procedure was repeated without affecting the sizes of the supraspheres and their ability to redisperse.

Received: June 13, 2007
Published online: September 27, 2007

Keywords: colloids · gold · nanostructures · solid-state reactions · surface chemistry

[1] C. J. Murphy, T. K. San, A. M. Gole, C. J. Orendorff, J. X. Gao, L. Gou, S. E. Hunyadi, T. Li, *J. Phys. Chem. B* **2005**, *109*, 13857 – 13870.
[2] L. R. Hirsch, R. J. Stafford, J. A. Bankson, S. R. Sershen, B. Rivera, R. E. Price, J. D. Hazle, N. J. Halas, J. L. West, *Proc. Natl. Acad. Sci. USA* **2003**, *100*, 13549 – 13554.
[3] W. R. Premasiri, D. T. Moir, M. S. Klempner, N. Krieger, G. Jones, L. D. Ziegler, *J. Phys. Chem. B* **2005**, *109*, 312 – 320.
[4] S. S. Shankar, A. Rai, A. Ahmad, M. Sastry, *Chem. Mater.* **2005**, *17*, 566 – 572.
[5] Y. G. Sun, Y. N. Xia, *Science* **2002**, *298*, 2176 – 2179.
[6] B. Nikoobakht, M. A. El-Sayed, *Chem. Mater.* **2003**, *15*, 1957 – 1962.
[7] C. X. Kan, X. G. Zhu, G. H. Wang, *J. Phys. Chem. B* **2006**, *110*, 4651 – 4656.
[8] C. C. Li, W. P. Cai, Y. Li, J. L. Hu, P. S. Liu, *J. Phys. Chem. B* **2006**, *110*, 1546 – 1552.
[9] X. P. Sun, S. J. Dong, E. K. Wang, *Chem. Lett.* **2005**, *34*, 968 – 969.
[10] H. C. Chu, C. H. Kuo, M. H. Huang, *Inorg. Chem.* **2006**, *45*, 808 – 813.
[11] J. E. Millstone, G. S. Metraux, C. A. Mirkin, *Adv. Funct. Mater.* **2006**, *16*, 1209 – 1214.
[12] J. Sharma, K. P. Vijayamohanan, *J. Colloid Interface Sci.* **2006**, *298*, 679 – 684.
[13] S. H. Chen, Z. Y. Fan, D. L. Carroll, *J. Phys. Chem. B* **2002**, *106*, 10777 – 10781.
[14] F. Kim, S. Connor, H. Song, T. Kuykendall, P. D. Yang, *Angew. Chem.* **2004**, *116*, 3759 – 3763; *Angew. Chem. Int. Ed.* **2004**, *43*, 3673 – 3677.
[15] P. D. Cozzoli, T. Pellegrino, L. Manna, *Chem. Soc. Rev.* **2006**, *35*, 1195 – 1208.
[16] J. Yang, H. I. Elim, Q. B. Zhang, J. Y. Lee, W. Ji, *J. Am. Chem. Soc.* **2006**, *128*, 11921 – 11926.
[17] H. Yu, M. Chen, P. M. Rice, S. X. Wang, R. L. White, S. H. Sun, *Nano Lett.* **2005**, *5*, 379 – 382.
[18] H. W. Gu, R. K. Zheng, X. X. Zhang, B. Xu, *J. Am. Chem. Soc.* **2004**, *126*, 5664 – 5665.
[19] By varying dilution at a constant [DT]/[NP] ratio, we were able to prepare SS whose sizes varied in the range 80–300 nm. These larger SS behave in the same way as those described and bud crystals upon heating.
[20] I. Hussain, Z. X. Wang, A. I. Cooper, M. Brust, *Langmuir* **2006**, *22*, 2938 – 2941.
[21] R. Klajn, K. J. M. Bishop, M. Fialkowski, M. Paszewski, C. J. Campbell, T. P. Gray, B. A. Grzybowski, *Science* **2007**, *316*, 261 – 264.
[22] R. Klajn, K. J. M. Bishop, B. A. Grzybowski, *Proc. Natl. Acad. Sci. USA* **2007**, *104*, 10305 – 10309.
[23] M. M. Maye, S. C. Chun, L. Han, D. Rabinovich, C. J. Zhong, *J. Am. Chem. Soc.* **2002**, *124*, 4958 – 4959.
[24] Although visible light has been reported to induce transformation of Ag nanoparticles into triangular prisms through plasmon excitation (cf. ref. [25]), these experiments required high irradiation power (150 W Xe lamp) and long irradiation times (ca. 50 h). In our system, the evolution of the SS was not affected by light, as confirmed by identical results of experiments conducted in the dark and in the daylight.
[25] R. C. Jin, Y. W. Cao, C. A. Mirkin, K. L. Kelly, G. C. Schatz, J. G. Zheng, *Science* **2001**, *294*, 1901 – 1903.
[26] This purification was done by precipitating the SS from toluene with methanol (up to 20 vol% in toluene), washing the black precipitate two times with copious amount of toluene/MeOH 4:1 mixture and resuspending in the original volume of toluene.
[27] M. M. Maye, W. X. Zheng, F. L. Leibowitz, N. K. Ly, C. J. Zhong, *Langmuir* **2000**, *16*, 490 – 497.
[28] D. V. Leff, L. Brandt, J. R. Heath, *Langmuir* **1996**, *12*, 4723 – 4730.
[29] X. G. Liu, N. Q. Wu, B. H. Wunsch, R. J. Barsotti, F. Stellacci, *Small* **2006**, *2*, 1046 – 1050.
[30] S. I. Stoeva, V. Zaikovski, B. L. V. Prasad, P. K. Stoimenov, C. M. Sorensen, K. J. Klabunde, *Langmuir* **2005**, *21*, 10280 – 10283.
[31] J. E. Millstone, S. Park, K. L. Shuford, L. D. Qin, G. C. Schatz, C. A. Mirkin, *J. Am. Chem. Soc.* **2005**, *127*, 5312 – 5313.
[32] C. Lofton, W. Sigmund, *Adv. Funct. Mater.* **2005**, *15*, 1197 – 1208.
[33] C. H. B. Ng, W. Y. Fan, *J. Phys. Chem. B* **2006**, *110*, 20801 – 20807.
[34] Z. L. Wang, *J. Phys. Chem. B* **2000**, *104*, 1153 – 1175.
[35] G. A. Somorjai, *Chemistry in Two Dimensions: Surfaces*, Cornell University Press, London, **1981**.
[36] C. J. Zhong, J. Zak, M. D. Porter, *J. Electroanal. Chem.* **1997**, *421*, 9 – 13.
[37] M. S. El-Deab, T. Sotomura, T. Ohsaka, *J. Electrochem. Soc.* **2005**, *152*, C1 – C6.
[38] W. H. Yang, G. C. Schatz, R. P. Van Duyne, *J. Chem. Phys.* **1995**, *103*, 869 – 875.
[39] A. C. Arsenault, G. A. Ozin, *Nanochemistry: A Chemical Approach to Nanomaterials*, RSC, Cambridge, **2005**.

